Journal of Computational Mathematics, Vol.25, No.3, 2007, 337–349.

MODELING PHOTONIC CRYSTALS WITH COMPLEX UNIT CELLS BY DIRICHLET-TO-NEUMANN MAPS [*1)]

Yuexia Huang and Ya Yan Lu
(*Department of Mathematics, City University of Hong Kong, Kowloon, Hong Kong, China*
Email: yxhuang@math.cityu.edu.hk, mayylu@cityu.edu.hk)

Abstract

For a photonic crystal (PhC) of finite size, it is important to calculate its transmission and reflection spectra. For two-dimensional (2-D) PhCs composed of a square lattice of circular cylinders, the problem can be solved by an efficient method based on the Dirichlet-to-Neumann (DtN) map of the unit cell and a marching scheme using a pair of operators. In this paper, the DtN operator marching method is extended to handle 2-D PhCs with complex unit cells and arbitrary lattice structures.

Mathematics subject classification: 78A45, 65Z05.
Key words: Photonic crystal, Periodic structure, Diffractive grating, Dirichlet-to-Neumann map, Operator marching.

1. Introduction

In recent years, photonic crystals (PhCs) have attracted much attention due to their unusual ability to manipulate light [1]. Many applications of PhCs have been proposed and realized in experiments. Numerical simulations are essential to understand the basic properties of PhCs and to design and optimize related components and devices. PhCs give rise to a number of interesting and challenging mathematical problems. For an infinite PhC, it is important to calculate its band structure. For PhCs with point defects and line defects, it is necessary to calculate the defect modes. If the PhC is finite in one direction, we need to solve a scattering problem for each given incident wave. The more general PhC structures, such as waveguide bends and branches, give rise to challenging boundary value problems.

One important problem is to analyze the transmission and reflection of a given plane wave incident upon a PhC of finite size. This problem is usually studied for many frequencies to produce the transmission and reflection spectra. Existing numerical methods developed for diffraction gratings, such as the Fourier modal method [2-7] and the finite element method [8], can be used to solve this problem. Special methods that take advantage of the geometric simplicity of PhCs are often more efficient. The multipole method [9-14] is a semi-analytic method suitable for PhCs composed of a lattice of circular cylinders. The boundary integral equation method [15] also has some advantages, since it only solves the wave field on surfaces of the cylinders. To take advantage of the partial periodicity in the direction where the PhC is finite, the scattering matrix formalism [10] and Floquet mode expansions [12, 13] can be used. In a recent paper [16], we developed a Dirichlet-to-Neumann (DtN) operator marching method for two-dimensional (2-D) PhCs composed of a square (or rectangular) lattice of circular

[*] Received November 10, 2006; final revised February 3, 2007; accepted February 7, 2007.
[1)] This research was partially supported by a City University of Hong Kong research grant (Project No. 7001862).

cylinders. The method takes full advantage of the geometric simplicity of a typical PhC. It uses a cylindrical wave expansion to construct the DtN map of the unit cell and to march two operators from one side of the PhC to another. A discretization in the unit cell is completely avoided. Compared with the multipole and the boundary integral equation methods, the DtN marching method is simpler, since it does not need sophisticated lattice sums techniques.

In this paper, we extend the DtN operator marching method to 2-D PhCs with general lattice structures and complex unit cells. By a complex unit cell, we refer to a unit cell containing more than one possibly different cylinders. While a complex unit cell can be divided into a few sub-cells each containing only one cylinder, the PhC is not periodic on the scale of the sub-cells. The additional freedom associated with different types of sub-cells can be used to design new devices, such as the photonic crystal resonator arrays in [17]. For PhCs with complex unit cells, we develop a merging technique that computes the DtN map of the complex unit cell from the DtN maps of its sub-cells. We also develop a shifting strategy for arbitrary 2-D lattices. The method works particularly well for the important case of triangular lattices. The efficiency and accuracy of our method are illustrated by a number of numerical examples.

2. The DtN Operator Marching Method

We consider a two-dimensional (2-D) photonic crystal (PhC) that is infinite in the x-direction and finite in the y-direction. The structure is periodic in x with period L and limited in y for $0 < y < D$, where D is the width of the PhC. For $y < 0$ (the bottom) and $y > D$ (the top), we assume that the medium is homogeneous with constant refractive index n_b and n_0, respectively. For an incident wave given in $y > D$, the scattering problem is to calculate the reflected wave in $y > D$ and the transmitted wave in $y < 0$.

For the E-polarization, the z-component of the time-harmonic electric field, denoted by u in this paper, satisfies the following Helmholtz equation

$$\frac{\partial^2 u}{\partial x^2} + \frac{\partial^2 u}{\partial y^2} + k_0^2 n^2\, u = 0, \tag{2.1}$$

where $n = n(x, y)$ is the refractive index function and k_0 is the free space wavenumber. For a plane incident wave, the scattering problem can be formulated as a boundary value problem of Eq. (2.1) in the rectangular domain given by $0 < x < L$ and $0 < y < D$. For $y > D$, we have $u = u^{(r)} + u^{(i)}$, where $u^{(i)}$ and $u^{(r)}$ are the incident and reflected waves given by

$$u^{(i)}(x, y) = e^{i[\alpha_0 x - \beta_0 (y-D)]}, \quad u^{(r)}(x, y) = \sum_{j=-\infty}^{\infty} R_j e^{i[\alpha_j x + \beta_j (y-D)]}, \quad y > D, \tag{2.2}$$

where β_0 is positive and R_j is an unknown reflection coefficient. If we denote θ_0 the angle between the wave vector $(\alpha_0, -\beta_0)$ and the y-axis, then

$$\alpha_0 = k_0 n_0 \sin\theta_0, \quad \beta_0 = k_0 n_0 \cos\theta_0, \quad \alpha_j = \alpha_0 + \frac{2j\pi}{L}, \quad \beta_j = \sqrt{k_0^2 n_0^2 - \alpha_j^2}.$$

For $y < 0$, we have only a transmitted wave given by

$$u = u^{(t)}(x, y) = \sum_{j=-\infty}^{\infty} T_j e^{i[\alpha_j x - \gamma_j y]}, \quad \text{for} \quad y < 0 \quad \text{and} \quad \gamma_j = \sqrt{k_0^2 n_b^2 - \alpha_j^2},$$

where T_j is an unknown transmission coefficient. The periodicity of the structure in the x direction gives rise to the following quasi-periodic conditions:

$$u(L,y) = \rho\, u(0,y), \quad \frac{\partial u}{\partial x}(L,y) = \rho\, \frac{\partial u}{\partial x}(0,y), \tag{2.3}$$

where $\rho = e^{i\alpha_0 L}$. With a proper definition of two operators $\tilde{S}_0$ and $\tilde{S}_b$ [18, 16], the boundary conditions at $y = 0$ and $y = D$ can be written down as:

$$\frac{\partial u}{\partial y} = -i\tilde{S}_b\, u, \quad y = 0, \tag{2.4}$$

$$\frac{\partial u}{\partial y} = i\tilde{S}_0\, u - 2i\beta_0 e^{i\alpha_0 x}, \quad y = D. \tag{2.5}$$

As a standard diffractive optics problem, the boundary value problem (2.1)-(2.5) can be solved by many existing numerical methods [2-8]. However, most of these methods fail to take advantage of the geometric simplicity of photonic crystals, since they are not specially designed for these PhCs. The DtN operator marching method was originally developed for waveguide problems [19]. It relies on two operators Q and Y defined at any fixed y_* as

$$Q(y_*)u(x,y_*) = \frac{\partial u}{\partial y}(x,y_*), \quad Y(y_*)u(x,y_*) = u(x,0), \tag{2.6}$$

where u is an arbitrary solution of (2.1) satisfying (2.3) and (2.4). Condition (2.5) is excluded in the above definition. Thus, Q and Y are defined for the infinitely many solutions of (2.1) together with (2.3) and (2.4). The operator Q is the global DtN map which maps the Dirichlet data u to the Neumann data $\partial_y u$. The operator Y is the fundamental solution (FS) operator. The main idea is to march these two operators (which are approximated by matrices) from $y = 0$ to $y = D$. At $y = 0$, the boundary condition (2.4) gives rise to $Q(0) = -i\tilde{S}_b$. The definition of Y implies that $Y(0) = I$, where I is the identity operator. If we know $Q(D)$, then the condition (2.5) gives rise to the following equation for solving the total field at $y = D$:

$$[Q(D) - i\tilde{S}_0]\, u(x,D) = -2i\beta_0 e^{i\alpha_0 x}. \tag{2.7}$$

The reflected wave is obtained from subtracting the incident wave from the total wave field, that is

$$u^{(r)}(x,D+) = u(x,D) - u^{(i)}(x,D+) = u(x,D) - e^{i\alpha_0 x}. \tag{2.8}$$

To find the transmitted wave, we need the operator $Y(D)$. We have

$$u^{(t)}(x,0-) = u(x,0) = Y(0)\, u(x,D). \tag{2.9}$$

To present the marching scheme, we divide y as

$$0 = y_0 < y_1 < \cdots < y_m = D.$$

For a photonic crystal, the rectangular region $\Omega_j = \{(x,y) \mid 0 < x < L,\ y_j < y < y_{j+1}\}$ usually corresponds to a unit cell. To march the operator Q and Y from y_j to y_{j+1}, the reduced DtN map M is required. The operator M is defined by

$$M \begin{bmatrix} u_j \\ u_{j+1} \end{bmatrix} = \begin{bmatrix} M_{11} & M_{12} \\ M_{21} & M_{22} \end{bmatrix} \begin{bmatrix} u_j \\ u_{j+1} \end{bmatrix} = \begin{bmatrix} \partial_y u_j \\ \partial_y u_{j+1} \end{bmatrix},$$

where u is any solution of (2.1) and (2.3), $u_j = u(x, y_j)$, $\partial_y u_j = \partial_y u(x, y_j)$, etc. In the above, we have a 2×2 partition of the matrix operator M. Each block of M, i.e., M_{ij}, is an operator acting on functions of x (for $0 < x < L$). From the definitions of Q, Y and M, the following marching formulas can be easily derived [16]:

$$Q(y_{j+1}) = M_{22} + M_{21}[Q(y_j) - M_{11}]^{-1} M_{12}, \tag{2.10}$$

$$Y(y_{j+1}) = Y(y_j)[Q(y_j) - M_{11}]^{-1} M_{12}. \tag{2.11}$$

The operator M can be constructed from another DtN map Λ which is the DtN map of the unit cell Ω_j. Let Γ_j be the boundary of Ω_j. The operator Λ maps u on Γ_j to the normal derivative of u on Γ_j, where u is any solution of the Helmholtz equation (2.1). More precisely, we have

$$\Lambda \begin{bmatrix} u_j \\ v_{0j} \\ v_{1j} \\ u_{j+1} \end{bmatrix} = \begin{bmatrix} \partial_y u_j \\ \partial_x v_{0j} \\ \partial_x v_{1j} \\ \partial_y u_{j+1} \end{bmatrix},$$

where $v_{0j} = u(0, y)$, $v_{1j} = u(L, y)$ for $y_j < y < y_{j+1}$, $\partial_x v_{0j} = \partial_x u(0, y)$, etc. For rectangular unit cells, the normal derivative on the boundary is simply taken to be the partial derivative with respect to x or y. If we partition Λ as 4×4 blocks and use the quasi-periodic conditions (2.3) to eliminate v_{0j} and v_{1j}, we obtain [16]

$$M = \begin{bmatrix} \Lambda_{11} & \Lambda_{14} \\ \Lambda_{41} & \Lambda_{44} \end{bmatrix} + \begin{bmatrix} C_1 D_1 & C_1 D_2 \\ C_2 D_1 & C_2 D_2 \end{bmatrix}, \tag{2.12}$$

where C_1, C_2, D_1 and D_2 are operators given by

$$\begin{aligned} &C_1 = \Lambda_{12} + \rho\Lambda_{13}, \quad C_2 = \Lambda_{42} + \rho\Lambda_{43}, \\ &D_0 = \rho\Lambda_{22} + \rho^2\Lambda_{23} - \Lambda_{32} - \rho\Lambda_{33}, \\ &D_1 = D_0^{-1}(\Lambda_{31} - \rho\Lambda_{21}), \quad D_2 = D_0^{-1}(\Lambda_{34} - \rho\Lambda_{24}). \end{aligned}$$

For unit cells containing a single circular cylinder, a matrix approximation to Λ can be constructed from the cylindrical wave expansion for solutions of the Helmholtz equation [16]. If N collocation points are used for $0 < x < L$, the operators Q, Y and M_{ij} are all approximated by $N \times N$ matrices. Typically, accurate results can be obtained with $N < 10$.

3. DtN Map for Complex Unit Cells

In many situations, the basic period of a PhC is a combination of more than one circular cylinders. To distinguish from a unit cell containing only one cylinder, the basic period of such a PhC will be called a complex unit cell. We assume that there are no overlaps between the cylinders in the photonic crystal. A complex unit cell may comprise a number of sub-cells each containing one cylinder. The cylinders in a complex unit cell may have different radii, different refractive indices and different locations in the sub-cells.

The DtN map for such a complex unit cell can be obtained by merging the DtN maps of sub-cells. In the following, we first consider a complex unit cell containing two sub-cells S_1 and S_2 as shown in Fig. 3.1. Let Θ and Δ be the DtN maps of the sub-cells S_1 and S_2, respectively,

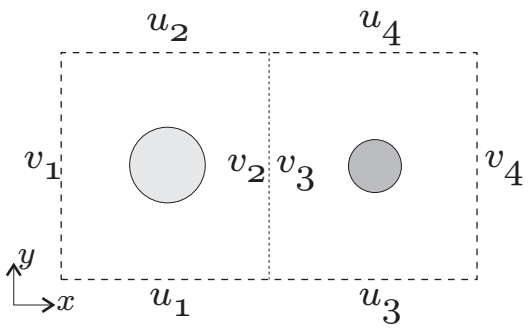

Fig. 3.1. A complex unit cell containing two sub-cells.

i.e.,

$$\Theta \begin{bmatrix} u_1 \\ v_1 \\ v_2 \\ u_2 \end{bmatrix} = \begin{bmatrix} \partial_y u_1 \\ \partial_x v_1 \\ \partial_x v_2 \\ \partial_y u_2 \end{bmatrix}, \quad \Delta \begin{bmatrix} u_3 \\ v_3 \\ v_4 \\ u_4 \end{bmatrix} = \begin{bmatrix} \partial_y u_3 \\ \partial_x v_3 \\ \partial_x v_4 \\ \partial_y u_4 \end{bmatrix}, \tag{3.1}$$

where u_j and v_j, for $1 \le j \le 4$, are the wave field u evaluated on the edges of the sub-cells. For the E polarization, both the field and its derivative are continuous. Therefore,

$$v_2 = v_3, \quad \partial_x v_2 = \partial_x v_3. \tag{3.2}$$

Using these conditions, v_2 or v_3 can be solved from the third equation of Θ and the second equation of Δ in (3.1). Inserting them into the remaining equations of (3.1), we obtain the following DtN map Λ for the complex unit cell:

$$\Lambda = \begin{bmatrix} \Theta_{11} & 0 & \Theta_{12} & 0 & \Theta_{14} & 0 \\ 0 & \Delta_{11} & 0 & \Delta_{13} & 0 & \Delta_{14} \\ \Theta_{21} & 0 & \Theta_{22} & 0 & \Theta_{24} & 0 \\ 0 & \Delta_{31} & 0 & \Delta_{33} & 0 & \Delta_{34} \\ \Theta_{41} & 0 & \Theta_{42} & 0 & \Theta_{44} & 0 \\ 0 & \Delta_{41} & 0 & \Delta_{43} & 0 & \Delta_{44} \end{bmatrix} + \begin{bmatrix} \Theta_{13} \\ \Delta_{12} \\ \Theta_{23} \\ \Delta_{32} \\ \Theta_{43} \\ \Delta_{42} \end{bmatrix} H^{-1} G,$$

where

$$H = \Delta_{22} - \Theta_{33}, \quad G = [\Theta_{31}, -\Delta_{21}, \Theta_{32}, -\Delta_{23}, \Theta_{34}, -\Delta_{24}].$$

The DtN map Λ acts on the column vector $(u_1, u_3, v_1, v_4, u_2, u_4)^T$. In the discrete case, the matrix $H^{-1}G$ above can be obtained by solving a linear system with the coefficient matrix H. Since the size of the matrices is typically quite small, the merging of two DtN maps can be done efficiently.

The DtN map for a complex unit cell containing more than two cylinders can be calculated by using the above algorithm repeatedly. For the H polarization and when the media outside the cylinders in the two sub-cells are different, the above merging step must be modified to take care of a different interface condition.

4. General Lattice Structures

In our previous work [16], the transmission and reflection spectra are calculated for PhCs composed of a square or a rectangular lattice. In that case, the rectangular domain Ω_j given

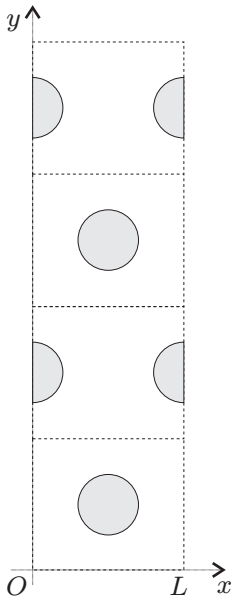

Fig. 4.1. The vertical strip Ω of a four layered triangular lattice.

by $0 < x < L$ and $y_j < y < y_{j+1}$ corresponds to a unit cell containing a cylinder at its center. A general infinite PhC has two translation vectors $\vec{a}_1$ and $\vec{a}_2$, such that

$$n(\vec{x}) = n(\vec{x} + p_1\vec{a}_1 + p_2\vec{a}_2), \tag{4.1}$$

where $\vec{x} = (x, y)$, p_1 and p_2 are arbitrary integers. In this paper, we assume $\vec{a}_1 = (L, 0)$ so that the structure is periodic in x with period L. For a non-rectangular lattice, the vector $\vec{a}_2$ is not parallel to the y-axis. One possible approach is to work on the parallelogram domain whose edges are parallel to $\vec{a}_1$ and $\vec{a}_2$, respectively. In that case, the domains Ω_0, $\Omega_1, \cdots$, are identical parallelogram unit cells. However, an accurate DtN map of such a unit cell is difficult to obtain due to the loss of a symmetry. Besides, the x-derivative, rather than the true normal derivative, must be used on the oblique edges, since we need to make use of the quasi-periodic conditions.

We choose to work on the vertical strip Ω given by $0 < x < L$ and $0 < y < D$ even for a non-rectangular lattice. In this case, the rectangular unit cell Ω_j (for $y_j < y < y_{j+1}$) may contain separated partial cylinders as shown in Fig. 4.1. For the important special case of a triangular lattice with $\vec{a}_2 = (L/2, \sqrt{3}L/2)$, there are only two different types of cells: the standard one with a cylinder at the center and the other one with two half-cylinders attached to the vertical edges. If we approximate the DtN map Λ of Ω_1 (the second unit cell from bottom in Fig. 4.1), the result may not be satisfactory, since the vertical edges intersect with the cylinders. However, we notice that Ω_1 is just a horizontal translation of a standard unit cell containing the cylinder at its center. Furthermore, the DtN map Λ is not directly used in the operator marching scheme. In fact, it is only used (together with the quasi-periodic conditions) to obtain the reduced DtN map M. In the following, we show that the operator M for Ω_1 can be obtained from the corresponding operator of a standard unit cell directly.

Consider a general lattice vector $\vec{a}_2$ and the unit cell Ω_1 given by $0 < x < L$ and $y_1 < y < y_2$ as shown in Fig. 4.2. We look for the reduced DtN operator M that maps $[u_1, u_2]^T$

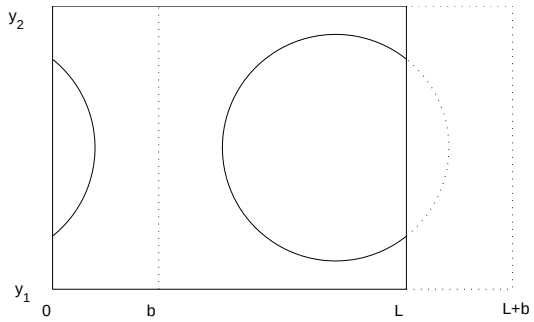

Fig. 4.2. The unit cell Ω_1 and its shifted cell $\tilde{\Omega}_1$.

to the y-derivative of u at y_1 and y_2, where $u_j = u(x, y_j)$ for $j = 1, 2$ and $0 < x < L$. Let $x = b \in (0, L)$ be the midpoint between two nearby cylinders, a standard unit cell $\tilde{\Omega}_1$ is obtained if we shift Ω_1 horizontally by a distance of b. More precisely, $\tilde{\Omega}_1$ is given by $b < x < L + b$ and $y_1 < y < y_2$. Using a column vector notation, we let $u_1 = [u_{11}, u_{12}]^T$ and $u_2 = [u_{21}, u_{22}]^T$, where $u_{j1} = u(x, y_j)$ for $0 < x < b$, $u_{j2} = u(x, y_j)$ for $b \le x < L$ and $j = 1, 2$. We also consider $L < x < L + b$ and let $u_{j3} = u(x, y_j)$ for $L < x < L + b$ and $j = 1, 2$. From the quasi-periodic conditions, we have

$$u_{j3} = \rho u_{j1}, \quad \text{for} \quad \rho = e^{i\alpha_0 L}.$$

Let $\tilde{M}$ be the reduced DtN map of the standard unit cell $\tilde{\Omega}_1$ satisfying

$$\tilde{M} \begin{bmatrix} u_{12} \\ u_{13} \\ u_{22} \\ u_{23} \end{bmatrix} = \frac{\partial}{\partial y} \begin{bmatrix} u_{12} \\ u_{13} \\ u_{22} \\ u_{23} \end{bmatrix}, \tag{4.2}$$

where $\partial_y u_{jk}$ denotes $\partial_y u$ evaluated at y_j in the corresponding interval of x. If we define an operator T such that

$$T \begin{bmatrix} u_{j1} \\ u_{j2} \end{bmatrix} = \begin{bmatrix} u_{j2} \\ \rho u_{j1} \end{bmatrix} = \begin{bmatrix} u_{j2} \\ u_{j3} \end{bmatrix}, \quad j = 1, 2,$$

and insert the above into Eq. (4.2), we obtain

$$M = \begin{bmatrix} T & \\ & T \end{bmatrix}^{-1} \tilde{M} \begin{bmatrix} T & \\ & T \end{bmatrix},$$

where M satisfies

$$M \begin{bmatrix} u_1 \\ u_2 \end{bmatrix} = \frac{\partial}{\partial y} \begin{bmatrix} u_1 \\ u_2 \end{bmatrix}.$$

If we write down the operators M and $\tilde{M}$ in 2×2 blocks, we have

$$M_{ij} = T^{-1} \tilde{M}_{ij} T, \quad \text{for} \quad i, j = 1, 2. \tag{4.3}$$

In the discrete case, if N sampling points are used for $0 < x < L$, the functions u_1 and u_2 are approximated by column vectors of length N, the operators M_{ij}, $\tilde{M}_{ij}$ and T become $N \times N$ matrices. Furthermore, if the intervals $(0, b)$ and $(L, L + b)$ each contain N_1 sample points, then for each j, u_{j1} and u_{j3} are column vectors of length N_1 and u_{j2} is a column vector of length $N_2 = N - N_1$. The matrices T and T^{-1} correspond to simple permutations with scalings and their multiplications require $\mathcal{O}(N^2)$ operations.

5. Numerical Examples

To validate our method, we calculate the transmission and reflection spectra for a number of examples and compare our results with those published by other authors. We first consider an example studied by Kushta and Yasumoto in [20]. The structure consists of an array of dielectric cylinders, but there are two different kinds of cylinders and they are arranged periodically in the x direction as shown in Fig. 5.1. The radii of the large and smaller cylinders are $r_a = 0.3L$ and $r_b = 0.15L$, respectively, where L is the period in the x direction. A small and a large cylinders are grouped together as a pair with no distance between them. The gap between two nearby pairs is $0.1L$. The refractive indices of the larger and small cylinders are $n_{1a} = \sqrt{2}$ and n_{1b}, respectively. The background medium is air with a refractive index $n_0 = 1$.

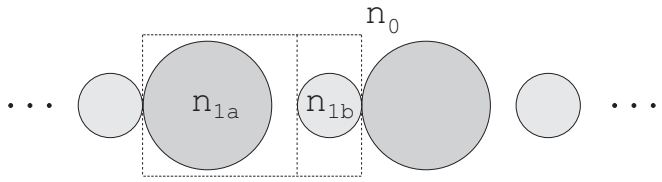

Fig. 5.1. An array of two different dielectric cylinders.

As indicated by the dashed lines in Fig. 5.1, we choose a complex unit cell containing two sub-cells with width $0.7L$ and $0.3L$, respectively. The sub-cells are separated by vertical lines which are tangent to the surfaces of the cylinders. The height of the unit cell is chosen to be $0.7L$. For this structure, we first calculate the DtN maps Λ_a and Λ_b for the two sub-cells following the cylindrical wave expansion technique described in [16], then combine Λ_a and Λ_b to obtain the DtN map Λ for the complex unit cell. After that, we calculate the reduced DtN map M and follow the operator marching scheme to find the transmission and reflection coefficients. In order to avoid the contact point of the two cylinders in a pair, we choose an even number of sampling points on the vertical edges. For the E polarization, we obtain the reflectivity curves of the structure for $n_{1b} = \sqrt{2}$ and $n_{1b} = \sqrt{2.5}$ as shown in Fig. 5.2. In these calculations, we have used 8 points on the vertical edges and $N = 12$ points on the horizontal edges of the complex unit cell. On the horizontal edges of the two sub-cells, the numbers of sampling points are 8 and 4, respectively. Our results are in good agreement with those obtained by Kashta and Yasumoto based on a sophisticated lattice sums technique [20]. Since the wave field near the contact points of the cylinders is quite complicated, a finite element method may require many elements to resolve the details.

For a general non-rectangular lattice, a shifting strategy for constructing the reduced DtN map M is presented in Section 4. To demonstrate the capability of this scheme, we consider an example first studied by Sakoda in [21]. The structure consists of a triangular lattice of air holes in a dielectric medium with the refractive index $n_2 = \sqrt{2.72}$. In the y direction, the dielectric medium is finite and there are 14 layers of air holes as shown in Fig. 5.3. The radius of the circular air holes is $0.431L$. The distance from the boundary of the background medium to the surface of the out-most layer of air holes is $0.778L$. For this problem, we use rectangular unit cells of size $L \times \left(\sqrt{3}/2\right) L$ as shown in Fig. 5.3. Notice that the horizontal lines separating different layers do not intersect with the air holes. In addition to the 14 layers containing the air holes, two more layers are needed to account for the extra dielectric medium beyond

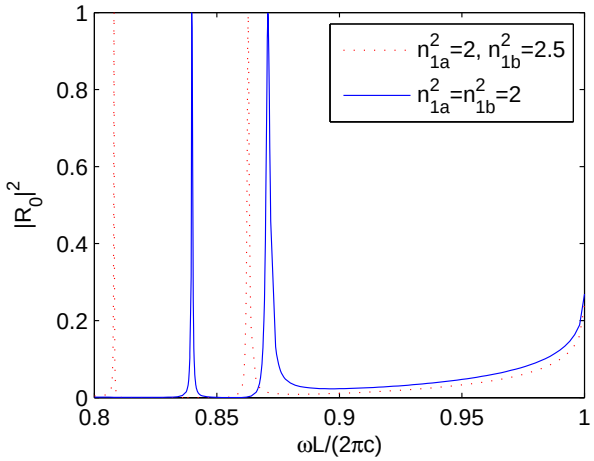

Fig. 5.2. Reflectivity of an array of two different dielectric cylinders.

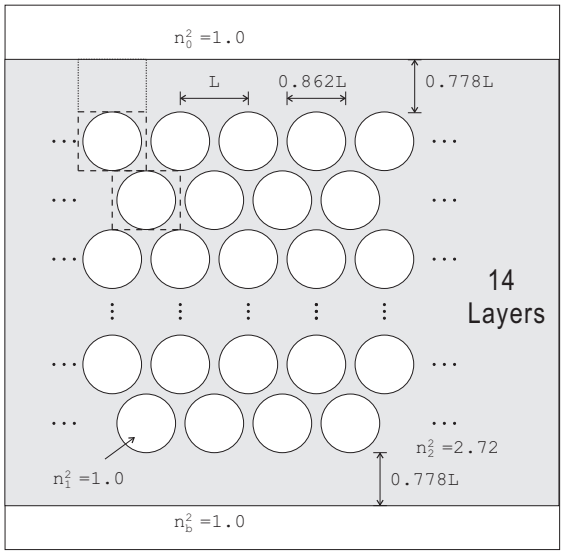

Fig. 5.3. A triangular lattice of air holes in a dielectric medium.

the out-most layers of air holes. Using our method with $N = 8$ and $N = 10$, we obtain the transmission spectrum of a plane incident wave shown Fig. 5.4. Our results agree with those of Sakoda [21], who used a plane wave expansion method with 1530 plane waves.

Finally, we consider a triangular lattice with two different types of cylinders. The structure was first analyzed by Amemiya and Ohtaka [22] using a cylindrical wave expansion method. As shown in Fig. 5.5, it consists of 24 layers of dielectric cylinders arranged in a triangular lattice of lattice constant L. The structure is periodic in the x direction with a period of $3L$. A complex unit cell of the structure is shown in Fig. 5.5 as the diamond region containing nine cylinders. The cylinders in the complex unit cell include eight small ones with radius $0.2L$ and one large cylinder with radius $0.3L$ at the center. The 24 layers of cylinders comprise 8 layers of the complex unit cells. The background medium is air ($n_2 = 1.0$). We denote the refractive indices of the smaller and lager cylinders by n_1 and n_{1c}, respectively.

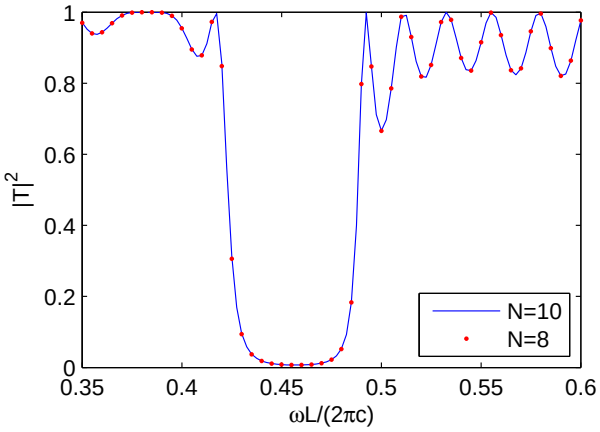

Fig. 5.4. Transmittance of a dielectric medium with 14 layers of air holes.

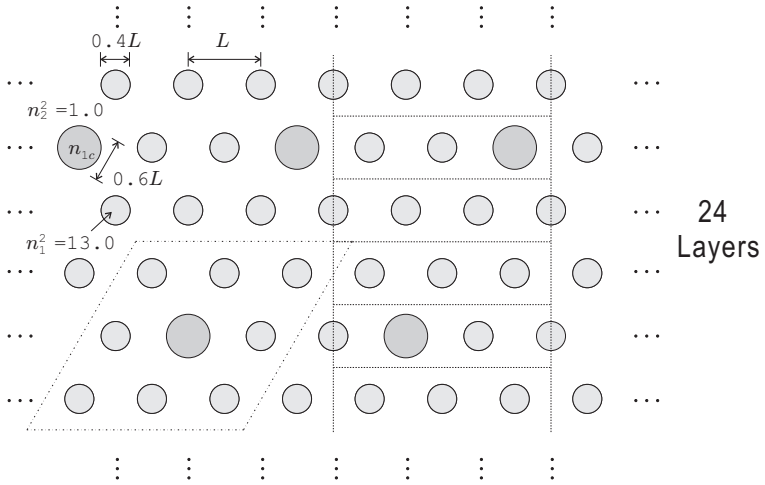

Fig. 5.5. A stack of two different dielectric cylinders in a triangular lattice.

In our implementation, we use the vertical strip Ω that covers one period in the x direction and all 24 layers in the y direction. Therefore, Ω is a rectangle of size $(3L)\times(12\sqrt{3}L)$. Although the structure has a complex unit cell containing three layers, it is easier to work with one layer a time. Let the 24 layers be separated by $y_j = j\sqrt{3}L/2$ for $j = 0, 1, 2, \cdots, 24$. To march the operators Q and Y from y_j to y_{j+1}, we need the reduced DtN map M for this layer. As shown in Fig. 5.5, the one-layer cell Ω_j given by $0 < x < 3L$ and $y_j < y < y_{j+1}$ contains either three small cylinders or one large and two small cylinders. Furthermore, a small cylinder may be replaced by two small half-cylinders. Using the merging technique described in Section 3, we can calculate the DtN map Λ for a one-layer cell containing three cylinders from the DtN maps of the sub-cells containing only one cylinder at its center. From the DtN map Λ, we can obtain the reduced DtN map M using the quasi-periodicity of the solution. Notice that ρ in Eq. (2.3) is now given by $\rho = e^{i3\alpha_0 L}$, since the period in x is $3L$. For the cells with half-cylinders attached to the vertical edges, we can construct the reduced DtN map M using the shifting technique described in Section 4. Since there are four different types of one-layer cells, the reduced DtN map M has four different cases.

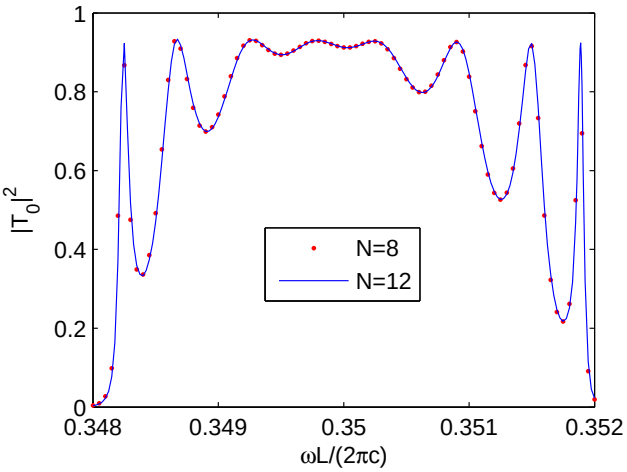

Fig. 5.6. Transmittance of 24 layers of two different dielectric cylinders in a triangular lattice with $n_1^2 = n_{1c}^2 = 13$.

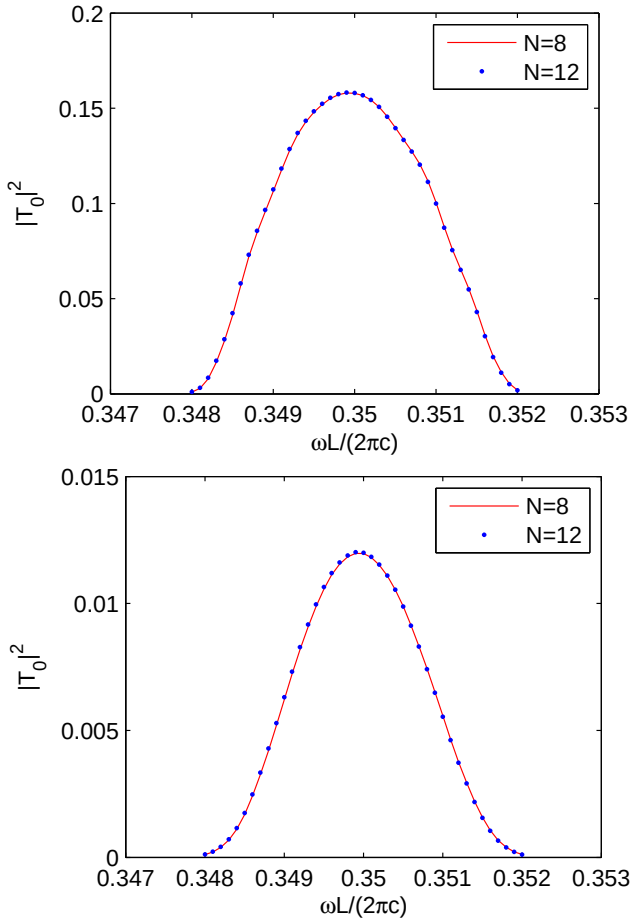

Fig. 5.7. Same as Fig. 5.6, except with $n_{1c}^2 = 13 + 0.02i$ (top) and $n_{1c}^2 = 13 + 0.05i$ (bottom).

For $n_1^2 = n_{1c}^2 = 13$, we calculate the transmission spectrum of this structure with $N = 8$ and $N = 12$, where N is the number of sampling points for a horizontal distance of L. The operators Q and Y are approximated by $(3N) \times (3N)$ matrices. Our results are shown in Fig. 5.6 and they agree well with those given in [22]. Next, we consider the effect of material loss in the large cylinders. The refractive index of the small cylinders is unchanged, but a small imaginary part is added to the dielectric constant n_{1c}^2 of the large cylinders. In Fig. 5.7, we show the transmission spectra for $n_{1c}^2 = 13 + 0.02i$ and $n_{1c}^2 = 13 + 0.05i$. Our results are consistent with those of Amemiya and Ohtaka [22].

6. Conclusion

Due to the periodicity of photonic crystals, it is possible to develop efficient algorithms that utilize the information of a unit cell to avoid repeated calculations on different cells. For two dimensional photonic crystals which are finite in one direction, we have previously developed such a method based on the Dirichlet-to-Neumann (DtN) map of a unit cell for computation of the transmission and reflection spectra [16]. The DtN map of the unit cell is also useful for band structure calculations [23]. The method in [16] deals with photonic crystals composed of a square or rectangular lattice of cylinders. In this paper, the method is extended to more complicated photonic crystals with a unit cell containing a number of possibly different cylinders (such a cell is referred to as a complex unit cell in this paper). We also present a practical method for handling general lattice structures. For a simple unit cell containing a circular cylinder, the DtN map can be constructed by a cylindrical wave expansion [16]. For non-circular cylinders, the DtN map can be calculated by a boundary integral equation method [24]. In Section 3, a merging technique is developed to find the DtN map of a complex unit cell. For a non-rectangular lattice, a simple shifting technique is developed for computing the reduced DtN map M. This allows us to solve the scattering problem in a rectangular domain covering one period of the structure in the infinite periodic direction.

The DtN map Λ of a unit cell can be used to derive the reduced DtN map M through an elimination process based on the quasi-periodicity of the wave field. The operator M is used to march the global DtN map Q and the fundamental solution operator Y from one side of the structure to another. The reflected and transmitted waves are then constructed from the final Q and Y. Due to the semi-analytic nature of these operators, they can be accurately approximated by small matrices. The size of these matrices is related to the number of sampling points on edges of the unit cells. Fast convergence as the number of sampling points increases was observed in [16]. In this paper, we obtain transmission and reflection curves that are in good agreement with those obtained by other authors using only a small number of sampling points.

References

[1] J.D. Joannopoulos, R.D. Meade and J.N. Winn, Photonic Crystals: Molding the Flow of Light, Princeton University Press, Princeton, NJ, 1995.

[2] J. Chandezon, M.T. Dupuis, G. Cornet and D. Maystre, Multicoated gratings - a differential formalism applicable in the entire optical-region, *J. Opt. Soc. Am.*, **72** (1982), 839-846.

[3] M.G. Moharam and T.K. Gaylord, Diffraction analysis of dielectric surface-relief gratings, *J. Opt. Soc. Am. A*, **72** (1982), 1385-1392.

[4] N. Chateau and J.P. Hugonin, Algorithm for the rigorous coupled-wave analysis of grating diffraction, *J. Opt. Soc. Am. A*, **11** (1994), 1321-1331.
[5] P. Lalanne and G.M. Morris, Highly improved convergence of the coupled-wave method for TM polarization, *J. Opt. Soc. Am. A*, **13** (1996), 779-784.
[6] L. Li, Formulation and comparison of two recursive matrix algorithms for modeling layered diffraction gratings, *J. Opt. Soc. Am. A*, **13** (1996), 1024-1035.
[7] L. Li, New formulation of the Fourier modal method for crossed surface-relief gratings, *J. Opt. Soc. Am. A*, **14** (1997), 2758-2767.
[8] G. Bao, Z.M. Chen and H.J. Wu, Adaptive finite-element method for diffraction gratings, *J. Opt. Soc. Am. A*, **22** (2005), 1106-1114.
[9] D. Felbacq, G. Tayeb and D. Maystre, Scattering by a random set of parallel cylinders, *J. Opt. Soc. Am. A*, **11** (1994), 2526-2538.
[10] R.C. McPhedran, L.C. Botten, A.A. Asatryan, et al., Calculation of electromagnetic properties of regular and random arrays of metallic and dielectric cylinders, *Phys. Rev. E*, **60** (1999), 7614-7617.
[11] L.C. Botten, N.A. Nicorovici, A.A. Asatryan, et al., Formulation for electromagnetic scattering and propagation through grating stacks of metallic and dielectric cylinders for photonic crystal calculations. Part I. Method, *J. Opt. Soc. Am. A*, **17** (2000), 2165-2176.
[12] L.C. Botten, T.P. White, A.A. Asatryan, et al., Bloch mode scattering matrix methods for modeling extended photonic crystal structures. I. Theory, *Phys. Rev. E*, **70** (2004), 056606.
[13] K. Yasumoto, H. Toyama and T. Kushta, Accurate analysis of two-dimensional electromagnetic scattering from multilayered periodic arrays of circular cylinders using lattice sums technique, *IEEE T. Antenn. Propag.*, **52** (2004), 2603-2611.
[14] K. Yasumoto, H. Jia and H. Toyama, Analysis of two-dimensional electromagnetic crystals consisting of multilayered periodic arrays of circular cylinders, *Electron. Comm. Jpn. 2*, **88** (2005), 19-28.
[15] S. Venakides, M.A. Haider and V. Papanicolaou, Boundary integral calculations of two-dimensional electromagnetic scattering by photonic crystal Fabry-Perot structures, *SIAM J. Appl. Math.*, **60** (2000), 1686-1706.
[16] Y. Huang and Y.Y. Lu, Scattering from periodic arrays of cylinders by Dirichlet-to-Neumann maps, *J. Lightwave Technol.*, **24** (2006), 3448-3453.
[17] H. Altug and J. Vuckovic, Two-dimensional coupled photonic crystal resonator arrays, *Appl. Phys. Lett.*, **84** (2004), 161-163.
[18] G. Bao, D.C. Dobson and J.A. Cox, Mathematical studies in rigorous grating theory, *J. Opt. Soc. Am. A*, **12** (1995), 1029-1042.
[19] Y.Y. Lu and J.R. McLaughlin, The Riccati method for the Helmholtz equation, *J. Acoust. Soc. Am.*, **100** (1996), 1432-1446.
[20] T. Kushta and K. Yasumoto, Electromagnetic scattering from periodic arrays of two circular cylinders per unit cell, *Prog. Electromagn. Res.*, **29** (2000), 69-85.
[21] K. Sakoda, Optical transmittance of a two-dimensional triangular photonic lattice, *Phys. Rev. E*, **51** (1995), 4672-4675.
[22] K. Amemiya and K. Ohtaka, Calculation of transmittance of light for an array of dielectric rods using vector cylindrical waves: complex unit cells, *J. Phys. Soc. Jpn.*, **72** (2003), 1244-1253.
[23] J. Yuan and Y.Y. Lu, Photonic bandgap calculations using Dirichlet-to-Neumann maps, *J. Opt. Soc. Am. A*, **23** (2006), 3217-3222.
[24] J. Yuan, Y.Y. Lu and X. Antoine, Modeling photonic crystals by boundary integral equations and Dirichlet-to-Neumann maps, submitted for publication.